

## Conduction Channel Transmissions of Atomic-Size Aluminum Contacts

E. Scheer, P. Joyez, D. Esteve, C. Urbina,\* and M. H. Devoret

*Service de Physique de l'Etat Condensé, Commissariat à l'Energie Atomique, Saclay, F-91191 Gif-sur-Yvette Cedex, France*

(Received 4 February 1997)

We have determined the individual transmission coefficients of Al quantum point contacts containing up to six conduction channels. The determination is based on a comparison of the highly nonlinear current-voltage characteristics in the superconducting state with the predictions of the theory for a single channel superconducting contact. We find that at least two channels contribute to the transport even for contacts with conductance lower than the conductance quantum. [S0031-9007(97)03088-3]

PACS numbers: 73.40.Jn, 74.50.+r, 73.20.Dx

In mesoscopic structures electrical transport takes place through independent “conduction channels” which are characterized by a transmission coefficient  $\tau_i$  and whose contribution to the total conductance  $G$  is  $G_0\tau_i$ , where  $G_0 = 2e^2/h$  is the conductance quantum [1]. An atomic-size constriction between two metallic electrodes can accommodate only a small number of such channels. The contact is thus fully described by a set  $\{\tau_i\} = \{\tau_1, \tau_2, \dots\}$ , which depends both on the chemical properties of the atoms forming the contact and on their geometrical arrangement [2–4]. Experimentally, contacts consisting of even a single atom have been obtained using both scanning tunnel microscope and break-junction techniques [5,6]. The total transmission  $\mathcal{T} = \sum_{i=1}^N \tau_i$  of the contacts is deduced from their measured conductance  $G$  using the Landauer formula  $G = G_0\mathcal{T}$ . Experiments on a large ensemble of metallic contacts have demonstrated the *statistical* tendency of atomic-size contacts to have a conductance  $G$  close to integer multiples of  $G_0$  [7–9]. Does this mean that each channel of the set is either fully open ( $\tau_i = 1$ ) or completely closed ( $\tau_i = 0$ ), i.e., that there is an underlying “transmission quantization”? This question cannot be answered solely by conductance measurements which provide no information whatsoever on the individual channels. We show in this Letter that the *full* set  $\{\tau_i\}$  is amenable to measurement in the case of superconducting materials.

Several authors [10–12] have calculated the current-voltage characteristics  $i(V, \tau)$  for a single channel superconducting contact with arbitrary transmission  $\tau$ . The upper left inset of Fig. 1 shows their numerical results [13]. A precise determination of the channel content of any superconducting contact is thus possible if one assumes that the total current  $I(V)$  results from the contributions of  $N$  independent channels,

$$I(V) = \sum_{i=1}^N i(V, \tau_i).$$

The  $i(V, \tau)$  curves present a series of sharp current steps at voltage values  $V = 2\Delta/ne$ , where  $n$  is a positive integer and  $\Delta$  is the superconducting gap. The well-known process of single quasiparticle transport corresponds to  $n = 1$ . The common phenomenon behind the other steps is multiple Andreev reflection (MAR) of quasiparticles

between the two superconducting banks [14]. The order  $n = 2, 3, \dots$ , of a step corresponds to the number of electronic charges transferred in the underlying MAR process. As the transmission of the channel rises from 0 to 1, the higher order processes grow stronger and the subgap current increases progressively. This so-called “subharmonic gap structure” has already been observed in superconducting weak links and tunnel junctions with a very large number of channels [15,16]. Measurements [17] of the current-voltage characteristic ( $IV$ ) of Nb and Pb single channel tunnel junctions with an adjustable transmission  $\tau_1$  have shown that the height of the successive current steps is proportional to increasing powers of  $\tau_1$ , in

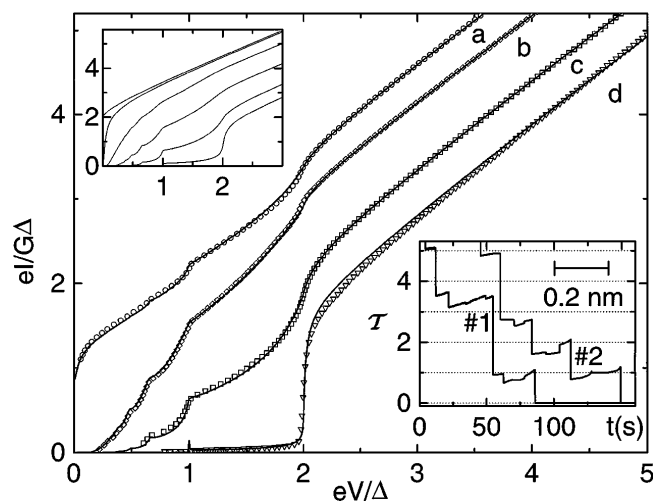


FIG. 1. Measured current-voltage characteristics (symbols) of four different configurations of sample #1 at 30 mK and best numerical fits (lines). The individual channel transmissions and total transmission  $\mathcal{T}$  obtained from the fits are (a)  $\tau_1 = 0.997$ ,  $\tau_2 = 0.46$ ,  $\tau_3 = 0.29$ ,  $\mathcal{T} = 1.747$ ; (b)  $\tau_1 = 0.74$ ,  $\tau_2 = 0.11$ ,  $\mathcal{T} = 0.85$ ; (c)  $\tau_1 = 0.46$ ,  $\tau_2 = 0.35$ ,  $\tau_3 = 0.07$ ,  $\mathcal{T} = 0.88$ ; and (d)  $\mathcal{T} = \tau_1 = 0.025$ . Voltage and current are in reduced units. The measured superconducting gap was  $\Delta/e = 182.5 \pm 2.0 \mu\text{V}$ . Left inset: Theoretical  $IV$ s for a single channel superconducting contact for different values of its transmission coefficient  $\tau$  (from bottom to top: 0.1, 0.4, 0.7, 0.9, 0.99, 1) after [12]. Right inset: Typical total transmission traces measured at  $V \geq 5 \Delta/e$ , while opening the contact at around 6 pm/s, for samples #1 and #2. The bar indicates the distance scale.

excellent agreement with the theory of MAR in the low  $\tau_1$  regime [18]. The same series of experiments, but in the contact regime, showed qualitatively that even for a single atom contact more than one conduction channel has to be considered. However, the transmission set  $\{\tau_i\}$  was not determined.

In order to infer  $\{\tau_i\}$  from the  $IV$ s, very stable atom-sized contacts are required. For this purpose we have used microfabricated mechanically controllable break junctions [19]. The break-junction technique was pioneered by Moreland and Hansma [20] and later developed by Muller *et al.* [21]. Our samples are  $2\ \mu\text{m}$  long,  $100\ \text{nm}$  thick suspended Al microbridges, with a  $100\ \text{nm} \times 100\ \text{nm}$  constriction in the middle (cf. Fig. 2). The bridge is broken at the constriction by controlled bending of the elastic substrate mounted on a three-point bending mechanism. A differential screw ( $100\ \mu\text{m}$  pitch), driven by a dc motor through a series of reduction gear boxes, controls the motion of the pushing rod that bends the substrate (Fig. 2). The geometry of the bending mechanism is such that a  $1\ \mu\text{m}$  displacement of the rod results in a relative motion of the two anchor points of the bridge of around  $0.2\ \text{nm}$ . This was verified using the exponential dependence of the conductance on the interelectrode distance in the tunnel regime. This very strong dependence was used to estimate the experimental interelectrode stability to be better than  $200\ \text{fm/h}$ . The bending mechanism is anchored to the mixing chamber of a dilution refrigerator. The bridges are broken at low temperatures ( $T < 1\ \text{K}$ ) and under cryogenic vacuum (obtained with a sorption pump) to prevent contamination of the two resulting elec-

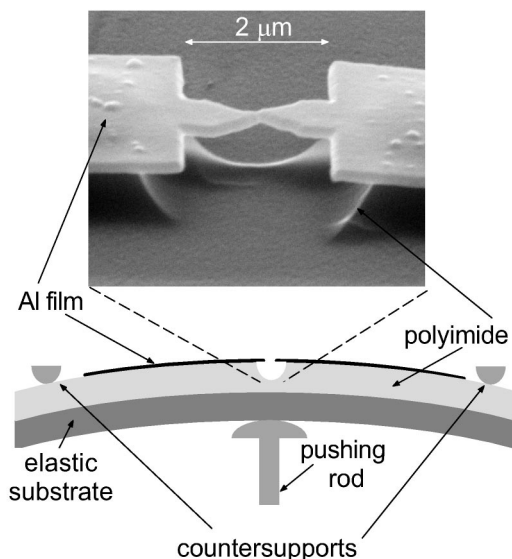


FIG. 2. Three-point bending mechanism. The pushing rod bends the phosphorbronze substrate. The distance between the two countersupports was  $12\ \text{mm}$ , and the substrate was  $0.3\ \text{mm}$  thick. The micrograph shows a suspended Al microbridge (sample #2). The insulating polyimide layer was etched to free the bridge from the substrate.

trodes. The voltage and the current through the device are measured using two low-noise differential preamplifiers. All lines connecting the sample to the room temperature electronics are carefully filtered by a combination of lossy coaxial and twisted pair cables [22], and microfabricated cryogenic filters [23]. We present in this Letter data obtained on three nominally identical samples.

After breaking, the electrodes are brought back into contact to form a point contact with a resistance of a few hundred ohms. Pushing again on the substrate leads to a controlled opening of the contact, while the sample is maintained at  $T < 100\ \text{mK}$ . As found in previous experiments at higher temperatures, the conductance  $G$  decreases in steps of the order of  $G_0$ , their exact sequence changing from opening to opening (see right inset of Fig. 1). Between two jumps,  $G$  generally tends to increase when pulling the contact. The last conductance value before the contact breaks is usually between  $0.5G_0$  and  $1.5G_0$ . We distinguish between contact and tunnel behavior by the different interelectrode distance dependence of the conductance in both regimes. The setup stability allows us to stop at any point along the breaking or closing curves in order to record the  $IV$ s. Figure 1 shows the  $IV$ s of four configurations obtained on sample #1 at  $T = 30\ \text{mK}$ . Note that curves 1(b) and 1(c) differ markedly even though they correspond to contacts

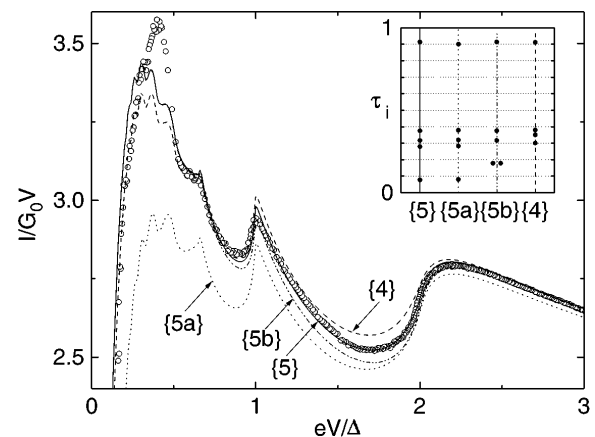


FIG. 3. Measured  $(I/V)$  (circles) as a function of voltage for a contact obtained on sample #3. We have used reduced quantities on both axes. Also shown are four calculated curves for different transmission sets  $\{\tau_i\}$ : {5}, five channel best fit,  $\mathcal{T} = 1.96$ ; {5a} and {5b}, five channel curves with slight deviations from best fit ensemble but the same  $\mathcal{T}$ ; {4}, four channel best fit,  $\mathcal{T} = 1.94$ . Inset: Set  $\{\tau_i\}$  for the four calculated curves. The set {5a} was obtained from {5} by reducing the transmission of the most transmitted channel by  $0.75\%$  of  $\mathcal{T}$ , and increasing the other four accordingly. The set {5b} was obtained from {5} by setting the transmissions of the two less transmitted channels to their average value, keeping the three others the same. The measured gap was  $\Delta/e = 185 \pm 2\ \mu\text{V}$ . The disagreement between experimental and theoretical curves below  $V = 2\Delta/4e$  is attributed to a resonance of the electromagnetic environment of the device [24] (see text).

having the same conductance within 5%. Curve 1(d) was obtained after the contact broke, i.e., in the tunnel regime, and is comparable to the results reported in [17]. When the device is driven into the normal state by applying a magnetic field  $B > B_c = 10$  mT, the  $IV$  becomes linear and corresponds to the same  $G$  as in the superconducting state far from the gap. When the magnetic field is turned off, we recover exactly the same  $IV$  as before.

In Fig. 1 we also show the best least-squares fits obtained using the numerical results of the  $T = 0$  theory [13]. The fitting procedure decomposes the total current  $I(V, \mathcal{T})$  into the contributions of six independent channels. Channels found with transmissions lower than 1% of the total transmission were neglected. Since the MAR processes start to contribute to the current at lower voltages as the order increases, we sampled the voltage with a density factor  $1/(V + V_0)$  with  $V_0 = 0.1\Delta/e$ . To illustrate the sensitivity of the fitting procedure, we show in Fig. 3 ( $I/V$ ) versus  $V$  for a particular contact on sample #3 along with four curves calculated with different  $\{\tau_i\}$ . Although  $\mathcal{T} \approx 2$ , a five channel fit is necessary in this case. Besides the five and four channels best fit curves we also show two curves obtained for slightly different values of the five individual transmission coefficients, keeping their sum constant (see inset of Fig. 3). When  $N \leq 3$ , this fitting procedure allows the determination of each  $\tau_i$

with an accuracy of 1% of  $\mathcal{T}$ . For contacts containing more channels only the two or three dominant channels (depending on their absolute value) can be extracted with that accuracy: As the number of contributing channels increases, or the transmission of some individual channels approaches  $\tau_i = 1$ , the information necessary to disentangle the contributions of additional channels is found in higher order MAR. Consequently, reliable data at lower voltages become increasingly important to obtain accurate fits. Experimentally, it is not possible to measure the current at infinitesimally low voltages because there is a hysteretic switching to the zero-voltage superconducting state. This sets a limitation to the maximum number of channels and the minimum value of transmission one can precisely characterize by this method. We stress that the total number of channels (with  $\tau_i$  larger than 1% of  $\mathcal{T}$ ) is perfectly determined by the fit. Only the low transmission values become less accurate when increasing  $N$ . In practice, a second error source affects the method: There is a residual disagreement between experiment and theory for voltages smaller than  $2\Delta/4e \approx 100 \mu\text{V}$  (see Fig. 3). We attribute it to inelastic Cooper pair tunneling corresponding to the excitation of a resonant mode of the electromagnetic circuit in which the contact is embedded [24]. For the particular geometry of our samples there is a resonance at a voltage of  $60 \pm 10 \mu\text{V}$  which prevents

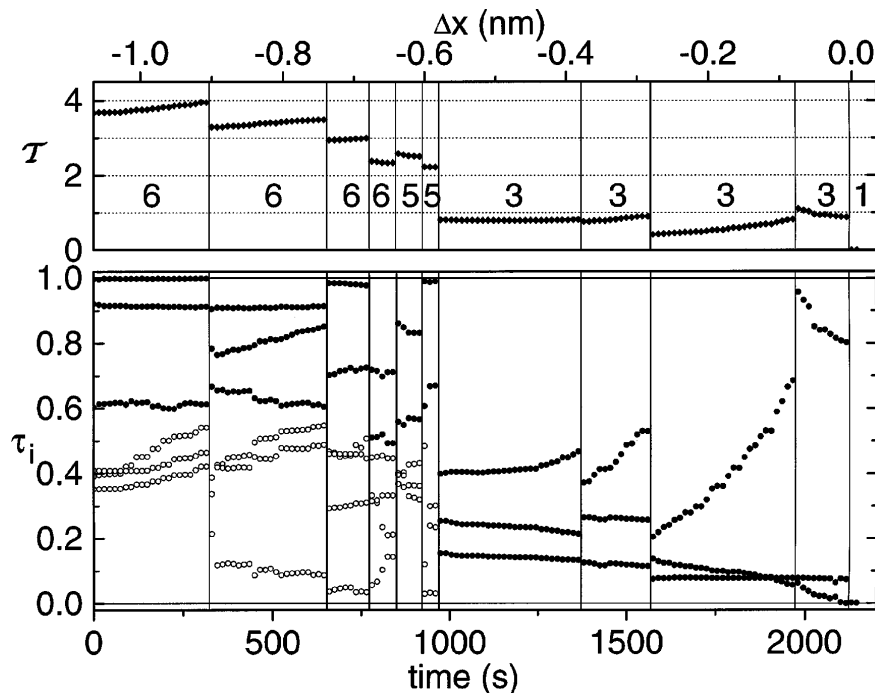


FIG. 4. Top panel: total transmission  $\mathcal{T} = \sum \tau_i$  as a function of time, as deduced from the best fit of the  $IV$ s recorded on flight while opening sample #3 at  $0.5 \text{ pm/s}$ . Bottom panel: evolution of individual transmission coefficients  $\tau_i$  as deduced from the fit; ( $\bullet$ ) channels determined with an accuracy of 1% or better of total transmission  $\mathcal{T}$ ; ( $\circ$ ) channels determined with an accuracy of 3% of  $\mathcal{T}$  or better. The vertical lines correspond to conductance jumps. For each region we have indicated the minimum number of channels necessary to fit the data. In the last contact before the jump to the tunnel regime three channels contribute significantly to the current. The upper  $x$  axis scale indicates the approximate variation of the distance between anchors. The origin of the distance axis has been set to the point where the contact breaks and enters the tunnel regime.

quantitative comparison below  $2\Delta/4e$ . However, proper design of the electromagnetic environment of the contact should eliminate this extrinsic limitation. We stress that although we present here data on contacts for which no more than six channels contribute, the method is in principle applicable for larger contacts.

The bottom panel of Fig. 4 shows in detail the evolution of  $\{\tau_i\}$  on sample #3, as the contact is opened. The upper panel of Fig. 4 shows the evolution of the total transmission  $\mathcal{T}$  as obtained from the sum of all individual transmissions. There are several remarkable features in this evolution. First, the abrupt changes in  $\mathcal{T}$  correspond generally to a *complete rearrangement* of the transmission set. Second, even during the more continuous evolution on the tilted plateaus the variations of  $\mathcal{T}$  arise from changes in *several* of the individual channels. Rubio *et al.* [25] proved that the jumps in *conductance* correspond to abrupt atomic rearrangements, and the tilted plateaus to elastic deformation of the contact. We can now extend their conclusions to the *transmission* of the *individual* conductance channels: The  $\tau_i$  are fully determined by the atomic configuration. These findings are consistent with the predictions of molecular dynamics calculations [26,27] and simplified models [28]. Third, the *number* of contributing channels does not always change when the total conductance changes abruptly. As shown in Fig. 4, some of the rearrangements of  $\{\tau_i\}$  do not involve the appearance (or the disappearance) of channels. The number of channels sequence shown in Fig. 4 is not universal: in particular, contacts with two or four active channels can also be found. Fourth, *more than one channel* contributes to the transport even for contacts with a total conductance lower than  $G_0$ . This is a general feature: once in the contact regime, we *never* find contacts that can be described by a single channel, even when  $G < G_0$ . In the case of Al, each atom contributes three orbitals to the conduction band and up to three channels can appear in a single atom contact [2,3]. Measurements on other superconductors are in progress.

In conclusion, our present work constitutes, first, a test of the theory for superconducting single channel contacts [10–12] for all values of the transmission coefficients. Second, it demonstrates that the set of the transmission coefficients in an atomic-sized contact is amenable to measurement. In the particular case of Al, we have shown that at least two conduction channels contribute to the current even in the smallest contact. More generally, we have established that even when the total conductance is close to an integer number  $N$  of conductance quanta, more than  $N$  channels contribute significantly to the current. In metals, “conductance quantization” does not necessarily mean “transmission quantization.” An intriguing question arises from our results: what makes atomic-sized contacts adopt, statistically, configurations with nearly integer values of conductance?

We acknowledge the technical assistance of P. F. Orfila, V. Padilla, and R. Silva, and enlightening discussions with K. W. Jacobsen, J. J. Sáenz, T. N. Todorov, and J. M. van Ruitenbeek. Finally, we have enjoyed fruitful interaction with D. Averin, J. C. Cuevas, and A. Levy Yeyati, and we thank them for providing us with their respective computer codes. This work was partially supported by the Bureau National de la Métrologie. E. S. acknowledges financial support by the Deutsche Forschungsgemeinschaft.

\*Electronic address: curbina@cea.fr

- [1] R. Landauer, IBM J. Res. Dev. **1**, 223 (1957); Philos. Mag. **21**, 863 (1970).
- [2] N. D. Lang, Phys. Rev. B **52**, 5335 (1995).
- [3] C. Sirvent *et al.*, Phys. Rev. B **53**, 16086 (1996).
- [4] P. García-Mochales *et al.*, Phys. Rev. B **53**, 1 (1996).
- [5] N. Agraït, J. C. Rodrigo, and S. Vieira, Phys. Rev. B **47**, 12345 (1993).
- [6] J. M. Krans *et al.*, Phys. Rev. B **48**, 14721 (1993), and references therein.
- [7] L. Olesen *et al.*, Phys. Rev. Lett. **72**, 2251 (1994).
- [8] J. M. Krans *et al.*, Nature (London) **375**, 767 (1995).
- [9] J. L. Costa-Krämer, N. P. García-Mochales, and P. A. Serena, Surf. Sci. **342**, L1144 (1995).
- [10] L. B. Arnold, J. Low Temp. Phys. **68**, 1 (1987).
- [11] D. Averin and A. Bardas, Phys. Rev. Lett. **75**, 1831 (1995).
- [12] J. C. Cuevas, A. Martín-Rodero, and A. Levy Yeyati, Phys. Rev. B **54**, 7366 (1996).
- [13] The three works [10–12] deal, through different approaches, with the same physics and provide essentially the same results for the *IV*. We have used the numerical results provided by [12] in order to draw the inset of Fig. 1 and to perform the fits.
- [14] Magnus Hurd, Supriyo Datta, and Philip F. Bagwell, Phys. Rev. B **54**, 6557 (1996), and references therein.
- [15] K. Flensberg and J. Bindslev Hansen, Phys. Rev. B **40**, 8693 (1989).
- [16] A. W. Kleinsasser *et al.*, Phys. Rev. Lett. **72**, 1738 (1994).
- [17] N. van der Post *et al.*, Phys. Rev. Lett. **73**, 2611 (1994).
- [18] E. N. Bratus, V. S. Shumeiko, and G. Wendin, Phys. Rev. Lett. **74**, 2110 (1995).
- [19] J. M. van Ruitenbeek *et al.*, Rev. Sci. Instrum. **67**, 108 (1996).
- [20] J. Moreland and P. K. Hansma, Rev. Sci. Instrum. **55**, 399 (1984).
- [21] C. J. Muller, J. M. van Ruitenbeek, and L. J. de Jongh, Physica (Amsterdam) **191C**, 485 (1992).
- [22] D. C. Glattli *et al.*, J. Appl. Phys. **81**, 6 (1997).
- [23] D. Vion *et al.*, J. Appl. Phys. **77**, 2519 (1995).
- [24] T. Holst *et al.*, Phys. Rev. Lett. **73**, 3455 (1994).
- [25] G. Rubio, N. Agraït, and S. Vieira, Phys. Rev. Lett. **76**, 2302 (1996).
- [26] T. N. Todorov and A. P. Sutton, Phys. Rev. Lett. **70**, 2138 (1993).
- [27] Uzi Landman *et al.*, Phys. Rev. Lett. **77**, 1362 (1996).
- [28] J. A. Torres and J. J. Sáenz, Phys. Rev. Lett. **77**, 2245 (1996).